Contrib. Plasma Phys. **53**, No. 1, 75 – 80 (2013) / **DOI** 10.1002/ctpp.201310013

Transient Plasma Measured by Fixed Electric Probes in the Scrape-Off Layer of Korean Superconducting Tokamak Advance Research (KSTAR)

Y.-S. Oh[1], **J.-G. Bak**[2,], **H.-J. Woo**[1], **E.-K. Park**[1], **H.-S. Kim**[2], **S.-G. Cho**[1], **S.-J. Park**[1], **T. Lho**[1,2,], and **K.-S. Chung**[1]*

[1] Department of Electrical Eng. & Center for Edge Plasma Science, Hanyang University, Seoul, Koera
[2] National Fusion Research Institute, Daejeon, Korea

Received 29 November 2011, revised 14 May 2012, accepted 03 October 2012
Published online 09 January 2013

Key words Ion saturation current, plasma flow, Mach probe, transient phenomena, KSTAR.

Transient plasma behavior in the scrape-off layer(SOL) is analyzed based upon the ion saturation current data measured by ninety-one fixed electric probes during the second and third campaigns of Korean Superconducting Tokamak Advance Research(KSTAR) operations ($2010 \sim 2011$). Experiments are implemented under the following conditions: plasma current of 600 kA, line average density of $6.1\times10^{19}\mathrm{m}^{-3}$, Neutral Beam Injection(NBI) power of 1.5 MW, and injection gas of D_2. Probes are made of carbon fiber composite(CFC) with a dome shape structure, and extruded about 1 mm from the surface of the background graphite tiles, which are exposed to the strongly magnetized plasma with an incident angle of the particles impinging on the probe from zero to nine degrees. Probes are installed in the limiter and divertor area of the KSTAR device with a bias voltage of -315 V in order to measure ion saturation currents. The ion saturation currents from the probes could identify the edge localized mode (ELM) phenomena comparing with D-alpha signals. In the distribution of the ion saturation currents measured by a probe array during a diverted plasma discharge process, it is found that two strike points move vertically upward and poloidally up and down at the inboard and central divertors, respectively. A comparative study of plasma behavior measured by electric probes is performed with the theoretical predictors of Equilibrium FITing code (EFIT) data.

1 Introduction

Given the large power expected from a plasma reactor, such as International Thermonuclear Experimental Reactor(ITER), divertor targets require additional cooling options to dissipate the significant power. By creating cold and dense plasma in the divertor, it is possible to access the detached regime whereby atomic loss mechanisms reduce the particle and power fluxes to the target plates [1]. The function of a magnetic divertor is to provide heat and particle exhaust and shield the main plasma from impurity contamination [2,3]. The target plates should survive for long-period plasma operations of the superconducting tokamak, and also transient phenomena such as ELM or disruptions. To avoid divertor damages, which is a critical issue in tokamak physics, it is necessary to reduce or distribute the heat flux at the strike points [4]. Important issues are still under debate: the particle transport in the SOL, the particle and heat flux to the wall, the transport of neutral particles and ions, and so forth [2]. During the KSTAR operation in $2010 \sim 2011$, various experiments have been carried out to characterize the ion saturation current, electron temperature, particle flux, and heat flux in the divertor region during the ELM phenomena, which are very important in fusion reactors due to the requirement of heat loads on plasma facing components in the divertor regions. Here we address the structure of fixed electric probes(EPs), the ion saturation currents measured during ELMs of KSTAR, and the deduction of heat fluxes. The probe data have been compared to the values simulated using Equilibrium FITing code (EFIT) with a good agreement. Most of the comparisons show consistent analysis results with a small portion of inconsistency.

* Corresponding author. E-mail: kschung@hanyang. ac.kr, Phone: +82 2 2220 4416, Fax: +82 2 2299 1908

2 Fixed electric probes

Transient plasma behavior in the SOL is analyzed based upon the measurement of ion saturation currents by ninety-one EPs during the operation of KSTAR. Figure 1 shows the geometrical structure, the cross-section view of the probes and the schematic of the possible phenomena. The probes represent a dome shape with a diameter of 6 mm. Figure 1 also shows a schematic overview of a fixed EP and its surrounding structure. The related physical processes to the given geometry of the probes around the divertor are explained in this scheme.

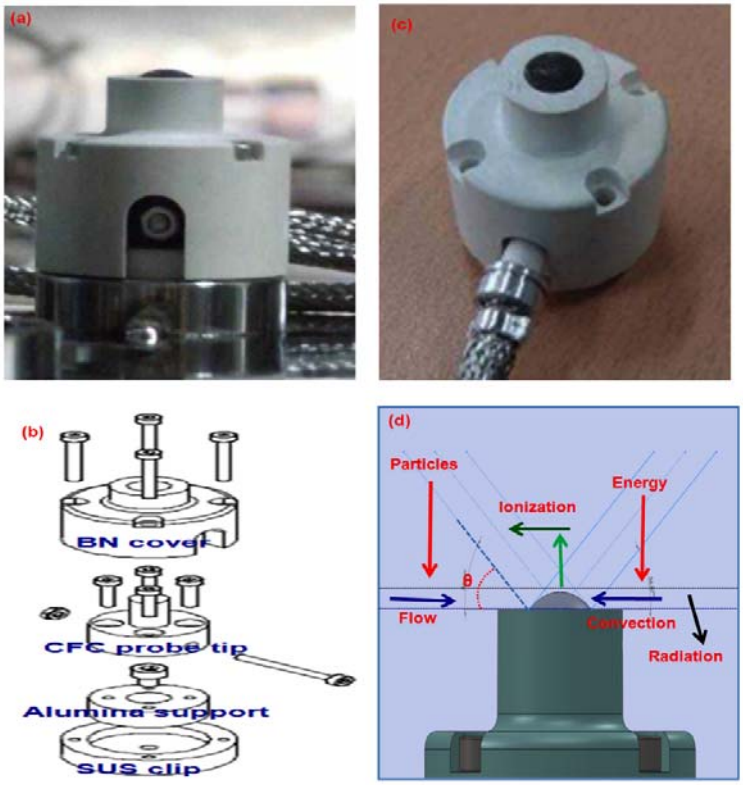

Fig. 1 (a),(b),(c),(d) Schematic overview of a fixed electric probe and the phenomena of the surrounding structures.

Ninety-one probes were installed along the peripheral line of the KSTAR vacuum vessel as shown in Figure 2. Twenty seven probes($EP36 \sim EP63$) analyzed in this study are located on the lower part of the vacuum vessel as shown in Figure 2. The projected areas and the incidence angles are calculated by considering the effective particles impinging on the probes, which is to be explained later, in Section 4, Deduced heat and particle fluxes. The projected area of the dome shaped probes should be calculated by considering the incidence angle to the reference baseline of the probe surface of surrounding tiles. Calculated areas are in the range of $4.09 \sim 6.91$ mm^2 according to the corresponding angles of $0 \sim 9.2$ degrees. Among 91 EPs, 9 probes are located in the inboard limiter, 23 are in the inboard divertor, 40 are in the central divertor, and 19 are in the outboard divertor. The axial locations(Z) from the height of KSTAR are $\pm 0.74 \sim \pm 1.04$ m, $\pm 1.13 \sim \pm 1.4$ m, and $\pm 0.97 \sim \pm 1.2$ m for the inboard divertor, central divertor, and outboard divertor, respectively. The radial locations(R) from the center of KSTAR are 1.26 m, $1.28 \sim 1.58$ m, and $1.75 \sim 1.57$ m for the lower inboard divertor, central divertor, and outboard divertor position, respectively. The incidence angle (degree) of a B field line is calculated using the toroidal (B_t) and poloidal (B_p) magnetic fields [3, 8]. The incidence angle varies from 0 to 9.2 degrees. The projected probe area of the probes in the poloidal direction varies from 4.09 to 6.91 mm^2 calculated in three-dimensional coordinate. These probe areas are calculated using the Math Cad programs and the area is proportional to the incidence angle.

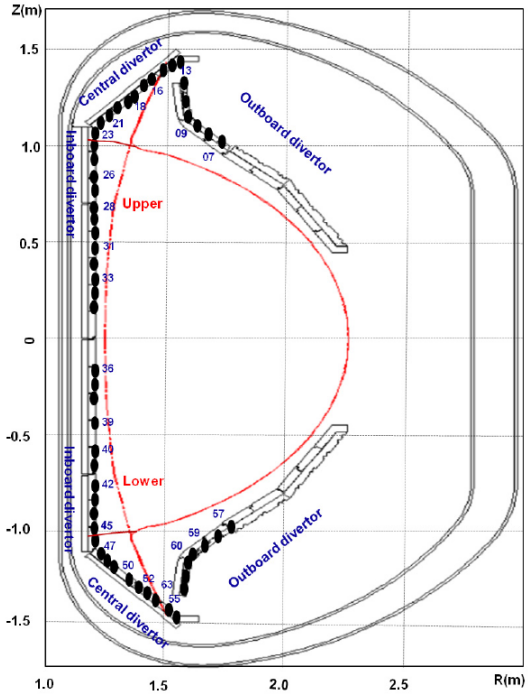

Fig. 2 Cross-section view of the EP arrays installed on the KSTAR (old probe: 2010)

3 Measured ion saturation currents

Figure 3 shows the plasma conditions of KSTAR: plasma current of 600 kA, line average density of $6.1 \times 10^{19}\mathrm{m}^{-3}$, neutral beam injection (NBI) with 1.5 MW, electron cyclotron heating (ECH) with 0.25 MW, loop voltage of 5 V, main injection gas of D_2, total stored energy of 200 kJ, electron cyclotron emission (ECE) with an 800 eV of edge region, and ELM phenomena occurred during $1.2 \sim 2.0$ s with D_α signals.

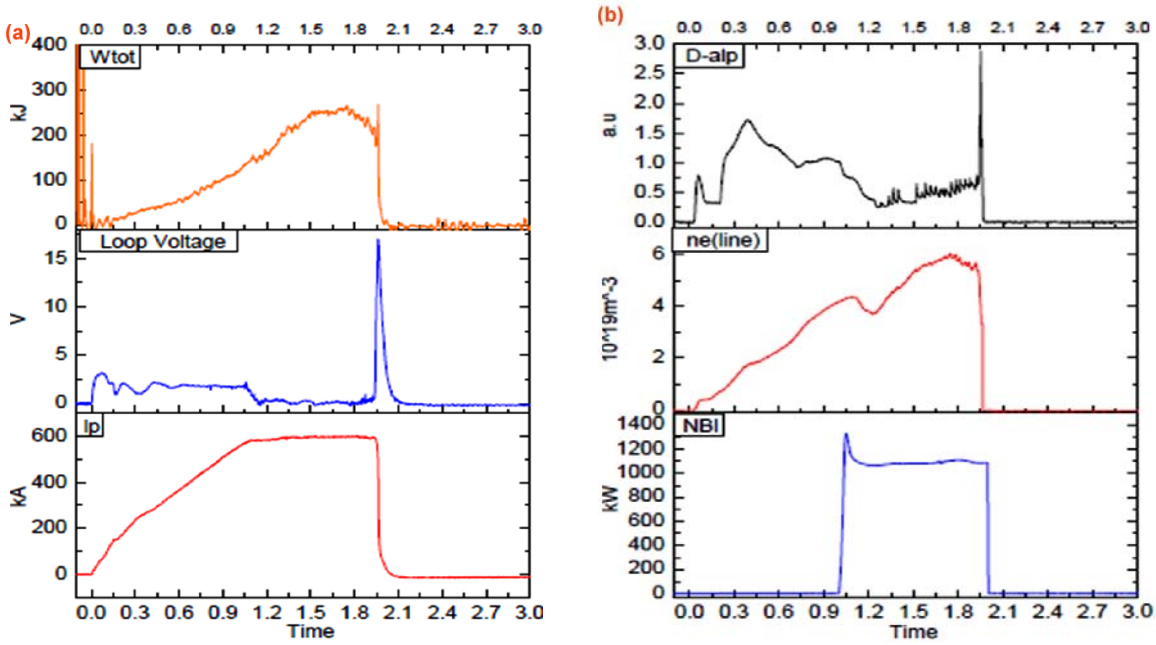

Fig. 3 Typical plasma conditions for our analysis (shot 4231). (a) W_{tot} (total store energy), and loop voltage and I_p (plasma current), (b) D_α signals, n_e (line average density) and NBI power.

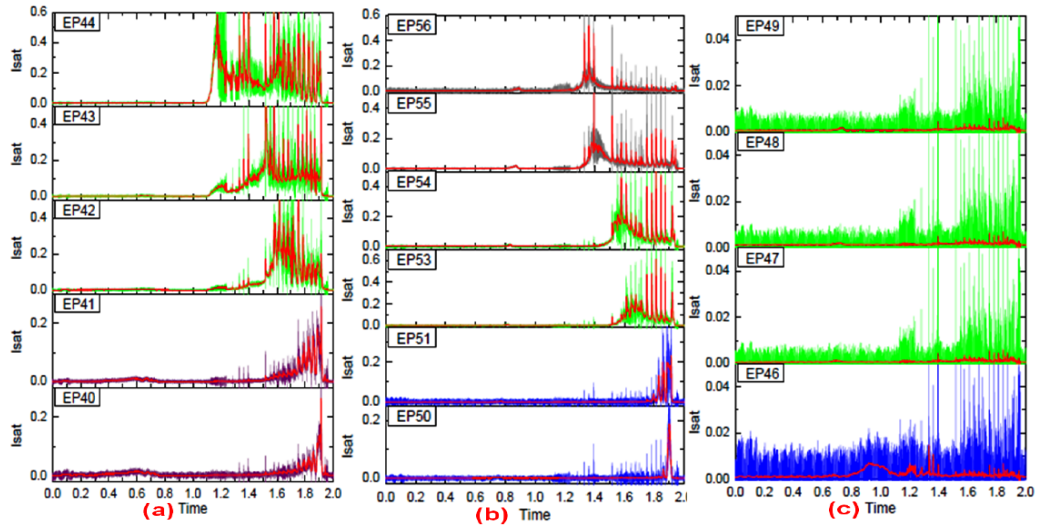

Fig. 4 Measured ion saturation currents by probes at the lower inboard divertor ((a)$EP40 \sim EP44$), and lower Central divertor ((b)$EP50 \sim EP56$: left side, (c)$EP47 \sim EP49$: right side), no significant change is shown for the probes at the lower outboard divertor.(shot 4231)

The ion saturation currents were measured by a bias voltage of -315 V to the probes in the limiter and divertor in the lower region of the KSTAR device. Figure 4 shows typical time evolution of the ion saturation current measured at the lower inboard divertor ($EP40 \sim EP46$), the central divertor ($EP47 \sim EP56$), and the outboard divertor ($EP57 \sim EP63$). The sampling frequency of the ion saturation current is 100 kHz. The maximum value of the time evolution in ion saturation currents near the strike point in the inboard and central divertors propagates in both directions (toward the inner and outer divertor), which might be caused by the different neutral pressures between the central divertor (higher) and the outboard divertor (lower). The neutral pressure of the private region (central divertor) around $EP46 \sim EP49$ seems to be higher than that of around $EP51 \sim EP55$.

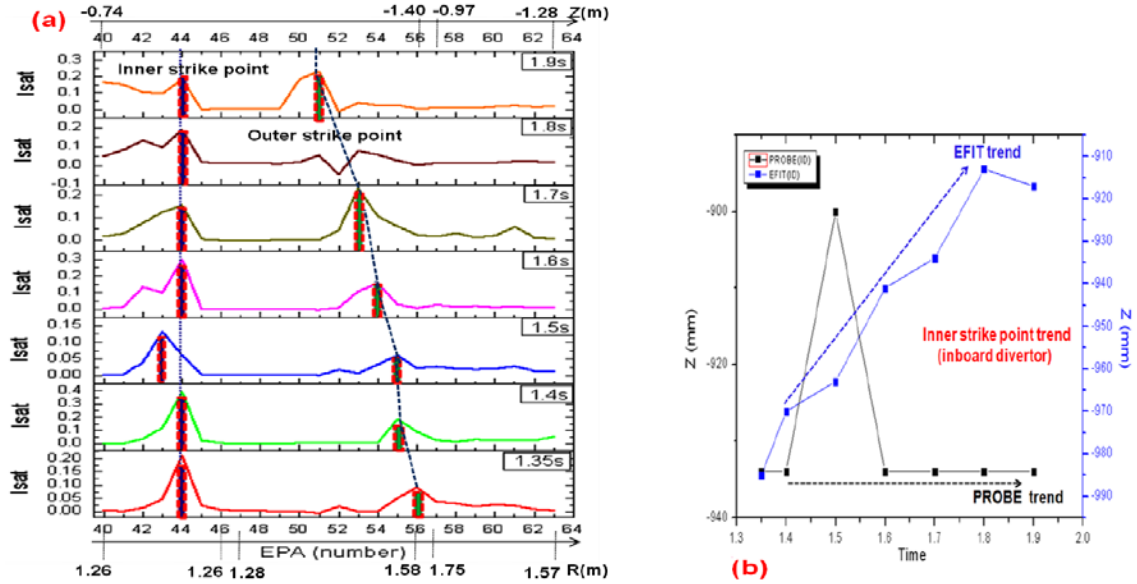

Fig. 5 Estimation of strike points deduced from the probe measurement via the EFIT simulation, (a) variation of strikes points during ELM bust peak points (radial locations(R): Fig 2), (b) The striking point is an inner strike point. The inner strike point represents trends of EFIT and PROBE in the inboard divertor.(shot 4231)

Figure 5 shows the estimated strike points, which are given by the probe measurement and the EFIT simulation. The strike points are varied during the ELM burst peak point. Inner strike points are located at the position of EPs of 43 and 44. Outer strike points are located at the position of EPs of 51 to 56, whose position are changing in the range of 210 to 240 mm. The strike point estimated by EFIT code seems to be in a good agreement with that measured by EPs. However, sometimes the estimation of EFIT and the data of the electric probes of inner strike point show different trends in time (Fig 5(b)). Measurement by EPs can be utilized to check the capability of shape control by EFIT estimations. One notices that strike points approach to the boundary between the inboard divertor and the central divertor where EPs of 46 to 48 are located, which indicates that high neutral pressure might lead to more active atomic processes. The electron pressure is lower at the inner strike point that is typical for the highly radiating conditions approaching detachment that are normally found without external pumping in the SOL [4].

4 Deduced heat flux and particle fluxes.

The parallel heat flux is decreased along the SOL from the upstream to the target. The divertor is a plasma facing component subject to the highest parallel heat flux. We operate the fixed probes in triple and single configurations depending on the plasma conditions in order to maximize the efficiency of the given probe profile. The triple configuration was used to measure floating potential(Φ_f), electron temperatures and ion saturation current(I_{sat}) at the lower outboart divertor of EPs 60,61, and 62(old probe: 2010) and EPs 118,119, and 120(new probe: 2011), among which EPs 60,61, and 118 compose one triple probe and EPs 62,119, and 120 compose the other. The single probes from one triple probe set are separated 1.7 cm poloidally and 6.6 cm toloidally. Thus, we assume that the separated probes would be located at the surface with the same plasma potential, leading to the deduction of electron temperature with spatial errors of 0.85 cm poloidally and 3.3 cm toloidally. The electron temperatures are ranged from 10 to 20 eV. The measurements of electron temperature and ion saturation currents were obtained separately by the triple configuration. Figure 6 shows the electron temperature measured during ELM phenomena in the triple configuration at the lower outboard divertor.

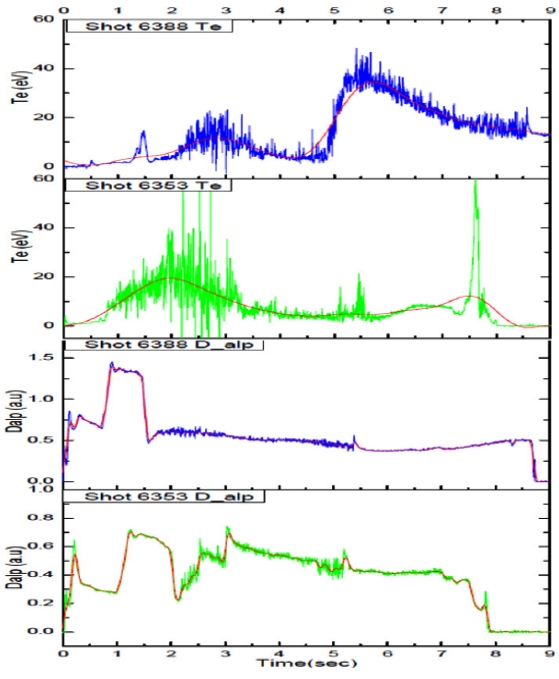

Fig. 6 Electron temperatures have measured during ELM phenomena of the triple configuration in the lower outboard divertor for various shots, which show the similar ranges in electron temperatures for various shots.

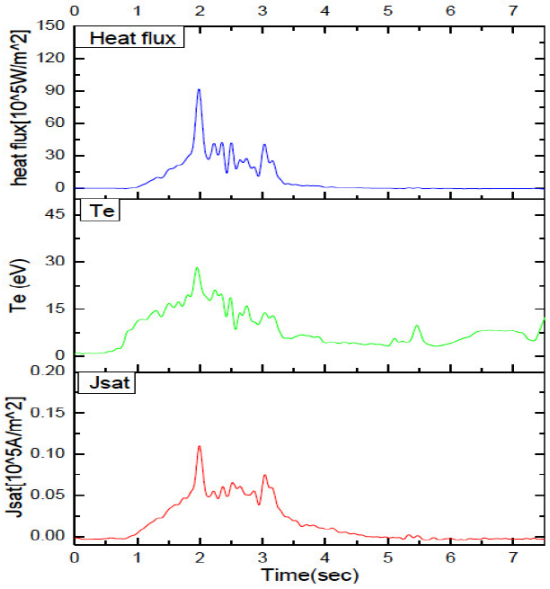

Fig. 7 Poloidal distributions of heat flux(Q) and particle fluxes, measured temperature, to the Outboard divertor fixed electric probes for the KSTAR shot 6353.

We deduced the ion saturation current density (J_{sat}) and heat flux (Q) at each probe position. The expression of the heat flux density from the plasma in given as $Q \equiv Q_i + Q_e = \gamma K T_e \Gamma$ [12,13]. Here we assumed that $T_i = T_e$ and $\Gamma = (J_s/e)$ where the value of γ is given as 6.5 in representing the hydrogen plasma total sheath heat transmission coefficient. Figure 7 shows the poloidal distribution of J_{sat} and Q. The value Q is decreased along both directions (to the inner and outer walls) at the outboard and central divertors while those at the inboard divertor are decreased to the upward direction.

5 Conclusion

Using fixed EPs, ion saturation currents, floating potentials and electron temperatures were measured at the lower divertor region of KSTAR device. EPs cross-section areas were calculated as $4.09 \sim 6.91$ mm^2 using the Math Cad Program. The ion saturation currents are consistent with J_{sat} and Q during ELM, assuming zero secondary electron emission. We can estimate the position of strike points using EFIT code as well as the fixed EPs that shows a good agreement. In some cases, such as transient plasma conditions, EFIT calculations present different temporal evolutions of the strike points compared with the probe measurements in ELM. The probe data can be used to correct the errors in EFIT simulations.

Acknowledgements This work is supported by the National R & D program through the National Research Foundation of Korea (NRF) funded by the Ministry of Education, Science and Technology (Grant number 2009-0082669 and 2012-0005926). This work is partially supported by the R & D program through the National Fusion Research Institute of Korea (NFRI) and the Korea Research council of Fundamental Science & Technology. It is also partially supported by the Brain Korea 21 (BK 21) program under the Ministry of Education, Science and Technology (MEST). Authors would like to thank S.-H. Hong , Y.-M. Jeon , J.-H. Kim, and S.-H. Hahn of the National Fusion Research Institute for their technical support.

.

References

[1] R.D. Monk, A. Loarte, A. Chankin, S. Clement, S.J. Davies, J.K. Ehrenberg, H.Y. Gou, J. Lingertat, G.F. Matthews, M.F. Stamp, and P.C. Stangeby, Journal of Nuclear Materials **241-243**, 369-401 (1997).
[2] J.A. Boedo, General Atomics Report **GA-A26173** (2009).
[3] J.A. Boedo, M.J. Schaffer, R. Maingi, C.J. Lasnier, and J.G. Watkins, Fusion and Plasma Phys. **23J**, 1185-1188 (1999).
[4] J.G. Watkins, R.A. Moyer, J.W. Cuthbertson, D.A. Buchenauer, T.N. Carlstrom, D.N. Hill, and M. Ulrickson, General Atomics Report **GA-A22362** (1996).
[5] I. Langmuir, Phys. Rev. **2**, 450 (1913).
[6] C. Child, Phys. Rev. **32**, 492 (1911).
[7] M. Weinlich and A. Carlson, Phys. Plasma **4**, 6 (1997).
[8] G.Y. Antar, S.I. Krasheninnikov, P. Devynck, R.P. Doerner, E.M. Hollmann, J.A. Boedo, S.C. Luckhardt, and R.W. Conn, American Physical Society **87**, 6 (2001).
[9] H. Miyoshi, N. Ohno, Y. Uesugi, N. Asakura, S. Takamura, and Y. Miura, Conference on Plasma Phys. **29C**, P-1.045 (2005).
[10] G.Y. Antar, G. Counsell, Y. Yu, B. Labombard, and P. Devynck, Fusion and Plasma Phys. **27A**, 172-175 (2003).
[11] J.L. Terry, S.J. Zweben, O. Grulke, M.J. Greenwald, and B. Labombard, Journal of Nuclear Materials **322-326**, 337-339 (2005).
[12] J. Wang, X. Gao, G. Xu, W. Zhang, J. Chang, H. Liu, W. Gao, Q. Zang, and T. Ming, Physica Scripta **78**, 035501-035506 (2008).
[13] P. Stangeby, "The Plasma Sheath", in Physics of Plasma-Wall Interaction in Controlled Fusion, ed., von D.F. Post and R. Behrisch, (Plenum, New York, 1986)

